Effects of Fermi Surface Anisotropy on Unconventional Superconductivity in UPt_3

G. Harań

Institute of Physics, Politechnika Wrocławska, Wyb.Wyspiańskiego 27, 50-370 Wrocław, Poland

P. J. Hirschfeld

Department of Physics, University of Florida, Gainesville, FL 32611, USA

and M. Sigrist*

Theoretische Physik, ETH, 8093 Zürich, Switzerland

(November 6, 1997)

Abstract

We discuss the weak-coupling BCS theory of the heavy fermion superconductor UPt_3, accounting for that system's anisotropic, multisheeted Fermi surface by expanding the order parameter and pair potential in terms of appropriate basis functions of the irreducible representations of the D_{6h} crystal point group. Within a phenomenological model for the electronic structure of UPt_3 chosen to capture the qualitative features of local density functional calculations and de Haas-van Alphen measurements, we show how Fermi surface anisotropy can favor pairing in certain symmetry classes, and influence the phase diagram of unconventional superconductors. We also calculate the Ginzburg-Landau coefficients, focussing on those coefficients relevant to current theories of the UPt_3 phase diagram.

I. INTRODUCTION

Several different scenarios have been proposed [1–5] to explain the unusual phase diagram of the heavy fermion superconductor UPt_3 in an external magnetic field [6,7] and under pressure. [8,9] This phase diagram consists of several superconducting phases of presumably different symmetry. Almost all theories of the phase diagram involve unconventional superconductivity, i.e. superconducting order parameters of lower symmetry than the conventional one which only breaks the U(1) gauge symmetry. These scenarios have almost exclusively been discussed on the basis of generalized Ginzburg-Landau (GL) theories of superconductivity, where the free energy functional is derived purely by symmetry arguments. [10–13] It is the nature of this approach that such theories require a considerable number of adjustable phenomenological parameters. In addition the choice of the order parameter, which can be classified according to the irreducible representations of the normal state symmetry group of the system, is open. Each representation corresponds to a Cooper pairing channel with a particular pairing energy, i.e. transition temperature.

At present, no satisfactory microscopic theory exists which could assist in picking out the relevant representation and fixing the phenomenological parameters of the corresponding GL theory. Of course, it is possible to work based on semimicroscopic formulation of a generalized weak-coupling BCS theory. This type of approach is often used in the study of properties related to the energy spectrum of the quasiparticle excitations for unconventional superconducting states with a specific topology of nodal structure of the quasiparticle gap, and considerable insight for various low-temperature properties has been gained from these treatments. [13] However, they are insufficient to answer the open questions we have in determining a GL theory. One difficulty arises from the fact that the specific form of the attractive pairing potential is unknown. Various additional corrections to the simplified weak-coupling treatment might be important and need to be properly taken into account. One aspect is the shape of the Fermi surface, (FS) which has multiple sheets, some of them very anisotropic. [14–16] In conventional weak-coupling calculations the FS has usually a

spherical symmetry. It would be helpful to connect the semimicroscopic and the GL approach by including effects of the FS anisotropy into the weak-coupling approach. Such effects are an important part in determining the symmetry of the relevant Cooper pairing channel as well as the values of the parameters in the GL theory, and have so far not been considered in the literature.

Let us now briefly review the situation in the theory of UPt_3. The scenarios for the UPt_3-phase diagram can be divided into three classes. (1) The relevant order parameter belongs to a two-dimensional (2D) representation of the crystal point group symmetry D_{6h} (hexagonal) of UPt_3, $E_{1(g,u)}$ or $E_{2(g,u)}$. [1,2,17,18] In this scenario a symmetry lowering field is required to lift the two-fold degeneracy of the 2D order parameter in order to describe the experimentally observed double transition. Such a field is given, for example, by the staggered moment of the weak antiferromagnetic order which appears below $T_N \approx 5K$ in UPt_3. [19] To this class of theories belongs in spirit an idea due to Zhitomirskii and Luk'yanchuk, [5] which states that the system is actually close to an isotropic one. Hexagonal anisotropy is then taken to split the representations of the rotation group, leaving nearly degenerate 1D or 2D representations. (2) The double transition can also occur for a triplet order parameter described by the one-dimensional (1D) representations of D_{6h} group, when the spin-orbit coupling interaction is negligible. In this model the degeneracy due to the spin direction is lifted by the staggered magnetic moment. [4,20] (3) It is also plausible, that two irreducible representations of D_{6h} might have their transition temperatures very close to each other (accidental near degeneracy) such that they would generate the feature of the double transtion. [3,5] The staggered moment does not play any role in this type of scenario.

As a test case for these scenarios usually the tetracritical point in the H-T-phase diagram of UPt_3 at $(H, T) \approx (500 Gauss, 0.4K)$ is analyzed. This point is most clearly observed for fields parallel to the basal plane, and is rather insensitive to the relative orientation with respect to the basal plane crystalline axes. The scenarios (1) have, in general, more difficulty than the scenarios (3) to reproduce this detail because of the anisotropy introduced by the staggered moment. One argument to overcome this flaw is the assumption that the staggered

moment always follows the orientation of the applied magnetic field. A further problem for the type 1) theories is that the observed tetracritical point for fields along the c-axis is not well reproduced. Sauls suggests that the problem could also be solved if certain parameters in the GL theory are very small. [1] Based on this idea he gave an argument in favor of the irreducible representation E_{2u} (f-wave) which is a triplet pairing state. Joynt [21] argues similarly that in an E_{1g} representation an apparent tetracritical point for $\mathbf{H} \parallel \hat{c}$ is obtained if the system is nearly particle-hole symmetric. The data for this configuration are not conclusive. [6] The scenarios (2) of the order parameter given by 1D representations and (3) which neglects the coupling between the staggered moment and the superconducting order parameter predict a tetracritical point in all directions.

Strong evidence in favor of theories (types 1) & 2)) which rely on the antiferromagnetic order as a symmetry breaking field is the observed simultaneous disappearance of both the high temperature, low field "A phase" and the staggered moment with the application of hydrostatic pressure. [8,9] The disappearance of the two transitions could be taken as evidence for the Zhitomirskii-Luk'yanchuk scenario, suggesting a nearness to "isotropy". However the simultaneous vanishing of the staggered magnetization seems more natural in the context of the 2D theories based on a symmetry breaking field. More recently, it was found that at the pressure value where the transitions merge, application of basal plane stress "resplit" the transition, lending further support to these scenarios. [22] On the other hand, in these theories the staggered magnetization generally must be assumed to rotate with the applied field in order to understand both the isotropy of the phase diagram for $\mathbf{H} \perp \hat{c}$ and the weak sixfold variation of the upper critical field H_{c2} with angle in the plane. [23] The recent experiment of Lussier et al. which found no rotation of the staggered moment with field appears to contradict this hypothesis, however. [24]

Further constraints on the theory are provided by recent Knight shift measurements, which show no temperature dependence for any direction of the field below T_c. [25] This striking result would be consistent with an equal spin pairing state such as in ^3He-A, with Cooper pair spins free to rotate with the external field. Such a model (type 3), in which

the order parameter is a spin triplet state with 3 spin components split by the staggered moment, has indeed been proposed by Machida and co-workers. [4,26] This theory has the disadvantage of generically exhibiting three transitions in zero field rather than two, due to the three independent order parameter components. It also cannot explain the apparent Pauli limiting of the upper critical field for $\mathbf{H} \parallel \hat{c}$. [27]

Thus, the existing experimental data have not been particularly kind to any of the current theoretical scenarios. It is not our aim to identify the correct theory here. Rather, we focus on an aspect which has been generally neglected in oversimplified models, namely which types of order parameter might be favored by the unusual, highly anisotropic Fermi surface of UPt_3. Within an extension of the semimicroscopic weak-coupling theory, we hope to be able to suggest which scenario is most likely, although no concrete proof can be given. From our analysis we expect to answer or shed light on some of the questions of interest. Are two nearly degenerate order parameters very likely to appear in UPt_3? Does the scenario (1) given by Sauls satisfy the conditions that GL theory would produce the isotropic tetracritical point? Is the system close to "isotropy" in the sense of Zhitomirskii and Luk'yanchuk? Which representations are favored by hexagonal anisotropy? And, how is the pairing potential distributed among the various sheets of the multisheeted Fermi surface?

Our discussion is considerably simplified by the assumption that a weak-coupling type of theory can be applied in case of UPt_3. Several properties of UPt_3 support the validity of such an approach. First, UPt_3 (in contrast to UBe_{13}) is in a rather well-developed Fermi liquid (FL) regime at the onset of superconductivity. For example, the linear specific heat and the T^2-dependence of the resistivity are suggestive for the existence of well-defined (Landau) quasiparticles. [14,28] Their effective mass is extremely large such that the degeneracy temperature T_F is of the order of $10 \sim 20K$. The question arises whether strong coupling effects are important in such a situation. They are measured by the ratio T_c/T_F which is here of the order of 1/20 . Thus we neglect these corrections, although they are considerably stronger than in conventional superconductors with $T_c/T_F \sim 10^{-3}$. Indirect justification for this assumption is provided by the size of the specific heat discontinuity at

the upper transition point, $\Delta C/C_N \sim 0.8$, [29] which has to be compared with the BCS weak-coupling result, $\Delta C/C_N \approx 1.43$. The FL renormalizations are of course quite large, as evidenced by the large effective mass. However, we will focus our attention to the properties of the superconductor close to the transition temperature, where these corrections are irrelevant. [30] Furthermore we simplify our discussion by taking the pairing potential as the only interaction among the quasiparticles into account. Thus the only modification to the usual weak-coupling theories is inclusion of the Fermi surface anisotropy. This implies also that pair correlation can be confined to a narrow energy shell about the FS of a width ω_c, the cutoff energy associated with the electron-electron interaction (analogous to the Debye frequency ω_D in conventional superconductors).

II. FERMI SURFACE ANISOTROPY AND THE CHOICE OF THE ORDER PARAMETER

A. The linearized gap equation

The BCS description of the superconductor is based on the following typical Hamiltonian

$$\mathcal{H} = \sum_{\mathbf{k},s} \varepsilon_{\mathbf{k}} c^{\dagger}_{\mathbf{k}s} c_{\mathbf{k}s} + \frac{1}{2} \sum_{\mathbf{k},\mathbf{k}'} \sum_{s_1,..,s_4} V_{s_1 s_2 s_3 s_4}(\mathbf{k},\mathbf{k}') c^{\dagger}_{-\mathbf{k}s_1} c^{\dagger}_{\mathbf{k}s_2} c_{\mathbf{k}'s_3} c_{-\mathbf{k}'s_4} \tag{1}$$

where $c^{\dagger}_{\mathbf{k}s}$ ($c_{\mathbf{k}s}$) denotes the creation (annihilation) operator of a quasiparticle with momentum $\mathbf{k}$ and spin s. The quasiparticle band $\varepsilon_{\mathbf{k}}$ is measured relative to the Fermi energy ε_F and $V_{s_1 s_2 s_3 s_4}(\mathbf{k},\mathbf{k}')$ is the pairing potential which is finite only for momenta $\mathbf{k}$ and $\mathbf{k}'$ for which $|\varepsilon_{\mathbf{k}}| < \omega_c$, $|\varepsilon_{\mathbf{k}'}| < \omega_c$, where only scattering processes between particles of opposite momentum are included. The superconducting state is expressed by the mean field

$$\Delta_{\mathbf{k}s_1 s_2} = -\sum_{\mathbf{k}'} \sum_{s_3,s_4} V_{s_1 s_2 s_3 s_4}(\mathbf{k},\mathbf{k}') \langle c_{\mathbf{k}'s_3} c_{-\mathbf{k}'s_4} \rangle \tag{2}$$

where $\langle ....\rangle$ is the thermal expectation value. The mean field $\Delta_{\mathbf{k}ss'}$ describes the gap of the quasiparticle spectrum $E_{\mathbf{k}} = [\varepsilon^2_{\mathbf{k}} + tr(\hat{\Delta}^{\dagger}_{\mathbf{k}} \hat{\Delta}_{\mathbf{k}})/2]^{1/2}$. The gap function $\hat{\Delta}_{\mathbf{k}}$ is a 2×2-matrix

in spin space. By inserting the expectation value for a given temperature T in Eq. (2) we obtain the self-consistency equation for the gap function,

$$\Delta_{\mathbf{k}s_1s_2} = -\sum_{\mathbf{k}'}\sum_{s_3,s_4} V_{s_1s_2s_3s_4}(\mathbf{k},\mathbf{k}')\frac{\Delta_{\mathbf{k}'s_3s_4}}{2E_{\mathbf{k}}}\tanh\left(\frac{E_{\mathbf{k}}}{2k_BT}\right) \tag{3}$$

This equation can be used to determine T_c by considering the limit of the order parameter amplitude $\Delta \to 0$ which yields the linearized gap equation

$$\nu\Delta_{\mathbf{k}s_1s_2} = -\sum_{\mathbf{k}'}\sum_{s_3,s_4} V_{s_1s_2s_3s_4}(\mathbf{k},\mathbf{k}')\Delta_{\mathbf{k}'s_3s_4}\delta(\varepsilon_{\mathbf{k}}) \tag{4}$$

where $1/\nu = \ln(1.14\omega_c/k_BT_c)$ is obtained by integrating $\tanh(\varepsilon/2k_BT_c)/2\varepsilon$ over ε in the energy shell, $-\omega_c < \varepsilon < \omega_c$. This equation is an eigenvalue equation where the largest among the eigenvalues ν determines the superconducting transition temperature T_c and the corresponding symmetry of gap function.

The Cooper pairing states can be classified into even (spin singlet) and odd (spin triplet) parity states which can be parametrized by a scalar function

$$\hat{\Delta}_{\mathbf{k}} = \Delta\psi(\mathbf{k})i\hat{\sigma}_y \tag{5}$$

for even parity and a vector function

$$\hat{\Delta}_{\mathbf{k}} = \Delta\sum_{\mu=x,y,z} d_\mu(\mathbf{k})i\hat{\sigma}_\mu\hat{\sigma}_y \tag{6}$$

for odd parity. If we assume that in the scattering described by $V_{s_1s_2s_3s_4}(\mathbf{k},\mathbf{k}')$ spins are not affected then the pairing potential has the following form

$$V_{s_1s_2s_3s_4}(\mathbf{k},\mathbf{k}') = \tilde{V}(\mathbf{k},\mathbf{k}')(\delta_{s_1s_3}\delta_{s_2s_4} \pm \delta_{s_1s_4}\delta_{s_2s_3}) \tag{7}$$

where the + (−)-sign occurs for $V_{s_1s_2s_3s_4}(\mathbf{k},\mathbf{k}')$ supporting odd (even) parity pairing. In this case the linearized gap equation can be expressed in the new parametrization as

$$\nu\psi(\mathbf{k}) = -\sum_{\mathbf{k}'}\tilde{V}(\mathbf{k},\mathbf{k}')\psi(\mathbf{k}')\delta(\varepsilon_{\mathbf{k}'}) \tag{8}$$

and

$$\nu d_\mu(\mathbf{k}) = -\sum_{\mathbf{k}'}\tilde{V}(\mathbf{k},\mathbf{k}')d_\mu(\mathbf{k}')\delta(\varepsilon_{\mathbf{k}'}) \tag{9}$$

Note that in the case of odd parity pairing the different components of $d_\mu(\mathbf{k})$ do not mix in the linearized gap equation.

B. Order parameter

In our weak-coupling approach we ignored quasiparticles further away from the FS so that in the linearized gap equation given in Eq. (4) the momentum sum is restricted to the Fermi surface. In this case we express the gap function in terms of the linear combinations of the spherical harmonics defined on an appropriate Fermi surface. It is however necessary to choose this set of polynomials $\{\phi_l(\mathbf{k})\}$ so that they are orthonormal to each other in the sense that the scalar product is determined as a FS average

$$\sum_{\mathbf{k}} \phi_l(\mathbf{k})\phi_{l'}(\mathbf{k})\delta(\varepsilon_{\mathbf{k}}) = \delta_{ll'} \tag{10}$$

where l is a label for the polynomial. This property is most easily achieved by classifying them with respect to the irreducible representations of the crystal field point group, D_{6h} in our case. Then only the polynomials within each irreducible representation have to be orthogonalized.

The gap function for the singlet state can now be written as

$$\psi(\mathbf{k}) = \sum_{l=1}^{n} \eta_l \phi_l(\mathbf{k}) \tag{11}$$

where η_l are the complex expansion coefficients. For the triplet state we have to express the vector $\mathbf{d}(\mathbf{k})$ which requires an additional set of polynomials $\{\varphi_l^{\mu}(\mathbf{k})\}$ which leads to

$$d_{\mu}(\mathbf{k}) = \sum_{l=1}^{n} \eta_{\mu l} \varphi_l^{\mu}(\mathbf{k}) \tag{12}$$

Orthogonality in this case is defined by

$$\sum_{\mathbf{k}} \sum_{\mu=x,y,z} \varphi_l^{\mu}(\mathbf{k})\varphi_{l'}^{\mu}(\mathbf{k})\delta(\varepsilon_{\mathbf{k}}) = \delta_{ll'} \tag{13}$$

In Tabs. I-III we catalogue these polynomials up to the order 3. We can now use them to express the linearized gap equation in matrix form as we show here for the case of even parity

$$\nu\eta_l = -\sum_{l'} \langle l|\tilde{V}|l'\rangle \eta_{l'} \tag{14}$$

where

$$\langle l|\tilde{V}|l'\rangle = \sum_{\mathbf{k},\mathbf{k}'} \delta(\varepsilon_{\mathbf{k}})\delta(\varepsilon_{\mathbf{k}'})\phi_l(\mathbf{k})\tilde{V}(\mathbf{k},\mathbf{k}')\phi_{l'}(\mathbf{k}') \tag{15}$$

Clearly, this eigenvalue equation decays into block form where each block belongs to one irreducible representation of D_{6h}. Thus we may consider the problem for each representation separately. There are representations in Tabs. I and III which have more than one polynomial. It is necessary to include all of them and ensure that they are orthonormalized. Note that the orthonormalization depends on the properties of the FS.

Sometimes it is advantageous to express the gap function in terms of so-called FS harmonics, as introduced by Butler and Allen, [31,32] and discussed in the context of the UPt_3 pairing problem in Ref. [33]. The Fermi surface harmonics are homogeneous polynomials of the Fermi velocity, $\mathbf{v_k} = \nabla_{\mathbf{k}}\varepsilon_{\mathbf{k}}$ and in the case of D_{6h} point group they can be obtained from Tabs. I-III by replacing $\mathbf{k}$ (k_i) by $\mathbf{v_k}$ (v_i). These functions are to be orthonormalized in the same way as the polynomials constructed from spherical harmonics. We will use the FS harmonic representation of the order parameter in Section 3 of this paper.

C. Pairing interaction and electron band

Now we have to specify the pairing interaction $\tilde{V}(\mathbf{k},\mathbf{k}')$ and the electron band $\varepsilon_{\mathbf{k}}$. In a spherical symmetric system the pairing states would be classified according to their angular momentum quantum numbers, ℓ and m (and radial quantum numbers among which we will consider here only the lowest ones in each angular momentum channel). States for a given ℓ are degenerate, i.e. yield in the linearized gap equation above the same transition temperature T_c. It is natural then to write the corresponding pair potential as

$$V_{s_1s_2s_3s_4}(\mathbf{k},\mathbf{k}') = \sum_{\ell} V_{\ell} \sum_{m=-\ell}^{+\ell} Y_{\ell m}(\mathbf{k})Y^*_{\ell m}(\mathbf{k}')[\delta_{s_1s_3}\delta_{s_2s_4} - (-1)^{\ell}\delta_{s_1s_4}\delta_{s_2s_3}] \tag{16}$$

where $Y_{\ell m}$ are the spherical harmonics depending on the Fermi vectors $\mathbf{k}$. Note that the $Y_{\ell m}(\mathbf{k})$ are dimensionless but are different from the usual $Y_{\ell m}(\hat{k})$ away from the isotropic

Fermi surface point. In this notation V_ℓ is negative for an attractive potential. In the following we will consider the FS anisotropy (crystal field) effects on the eigenvalues of Eq. (4). The information we can obtain is how the degenerate eigenstates evolve as the FS gradually becomes anisotropic. We will keep the interaction in this form where V_ℓ is an unknown parameter.

Information from experimental data as well as band structure calculation can help us to obtain an approximate electron band $\varepsilon_{\mathbf{k}}$. While the FS of UPt_3 is highly complex and consists of at least five sheets, [14–16] not all of them are equally important. We will focus here on two bands only which are supposed to be the ones with the largest and the third-largest contribution to the density of states, that is the Γ_3 and Γ_2 FS sheet respectively (notation from Ref. 16). A simple but crude fit of the band structure data can be achieved by the following form for $\varepsilon_{\mathbf{k}}$

$$\varepsilon_{\mathbf{k}} = a_1 k_z^2 + a_2(k_x^2 + k_y^2) + a_3(k_y^3 - 3k_x^2 k_y)^2 - \varepsilon_F \tag{17}$$

where a_i and ε_F are fit parameters. The Γ_2 band is fitted by an ellipsoidal $\varepsilon_{\mathbf{k}}$ which is rotationally symmetric about the c-axis, that is $a_3 = 0$ in Eq. (17). The hexagonal anisotropy is larger for the Γ_3 band which we approximate by a "wrinkled" ellipsoid with $a_3 \neq 0$. Note, that the latter band has additional pockets at Brioullin zone boundary which are not reproduced by $\varepsilon_{\mathbf{k}}$ from Eq. (17). However, this form of $\varepsilon_{\mathbf{k}}$ has the advantage that we can follow continuously the development of the anisotropic bands starting from a spherical symmetric one ($a_1 = a_2 \neq 0$ and $a_3 = 0$). The values of the parameters in $\varepsilon_{\mathbf{k}}$ for the anisotropic band are obtained using the ratios k_{F_x}/k_{F_z} and k_{F_y}/k_{F_z} from LDA calculations [16] and by conserving the area of cross section in the k_y-k_z plane as observed in de Haas-van Alphen measurements. [14] Our best fit parameters are given in Tab. IV, and the FS cross sections by the symmetry planes are shown in Fig. 1. This fit leaves still the density of states integrated over the FS as an undetermined parameter. In the following we will express various quantities in dimensionless units refering to the integrated density of states.

D. Solution of the linearized gap equation

We address now the problem of the stability of the possible pairing states in the given Γ_2- and Γ_3-band. In reality, superconductivity is a combined effect of all FS sheets, because quasiparticle scattering among the different sheets will couple their pairing amplitudes. It would be not difficult to introduce such interband coupling in the pairing interaction $\tilde{V}(\mathbf{k}, \mathbf{k}')$, but this would lead to additional unknown coupling parameters. In the following discussion we will avoid this complication and consider the effect of the two FS sheets separately as if they were uncoupled.

We investigate the effect of the FS anisotropy on the pairing states by continuously distorting a spherical FS into the above defined FS sheets Γ_2 or Γ_3 (Eq. (17)). For the spherical FS all pairing states of the same angular momentum ℓ are degenerate. The degeneracy of these $2\ell + 1$ states is lifted when the FS deviates from the spherical shape, and they can be classified by the irreducible representations of the new, lower symmetry D_{6h}. Restricting our attention to only one value of ℓ ($\ell = 1, 2$ and 3) at a time we need only to take one coupling parameter, V_ℓ, into account. This assumption may be too simplistic for realistic pair potentials, but we make it in the first analysis to isolate the effects of the Fermi surface anisotropy. We use an eigenvalue ν_ℓ of Eq. (4) on the spherical FS of the same integrated density of states, $N(0)$, as a reference value for ν. Expressed in dimensionless units $\nu' = \nu/\nu_\ell$ does not depend on $N(0)$, which is not determined within this approach. The distortion from a spherical FS that is the effect of a crystal field is included by the dimensionless linear parameter t changing from 0 to 1, with $t = 0$ corresponding to the spherical Fermi surface of the radius adjusted to dHvA data [14] and $t = 1$ representing Γ_3 or Γ_2 Fermi sheet (Tab. IV). Therefore an increase in t implies a higher hexagonal (Γ_3) or ellipsoidal (Γ_2) perturbation of the Fermi surface. The t-dependence of the energy band coefficients for the hexagonal FS is given by

$$
\begin{aligned}
a_1(t)/(\varepsilon_F c^2) &= 0.225 - 0.068t \\
a_2(t)/(\varepsilon_F c^2) &= 0.225 + 0.016t \\
a_3(t)/(\varepsilon_F c^6) &= 0.016t
\end{aligned}
\tag{18}
$$

and for the ellipsoidal Fermi sheet

$$
\begin{aligned}
a_2(t)/(\varepsilon_F c^2) &= 0.666 - 0.200t \\
a_2(t)/(\varepsilon_F c^2) &= 0.666 + 0.285t \\
a_3(t) &= 0
\end{aligned}
\tag{19}
$$

where c is the z-axis lattice constant (Tab. IV). The solutions of the linearized gap equation (Eq. (4)) for the p-wave, d-wave and f-wave pair potentials as the functions of the crystal field t are shown in Fig. 2 for the case of pairing interaction on Γ_3 Fermi sheet only (hexagonal crystal field) and Fig. 3 for the case of pairing potential on Γ_2 Fermi sheet (ellipsoidal crystal field). We present the critical temperature T_c for triplet states (Figs. 2a,2c,3a,3c) with $\mathbf{d} \parallel \hat{z}$ (Eq. (6)) only as the states with $\mathbf{d} \perp \hat{z}$ are degenerate with them according to Tabs. I and III. Particularly interesting is the result for the d-wave states with the pairing interaction on Γ_3 FS (Fig. 2b). We observe here a competition between A_{1g} and E_{1g} states as the hexagonal anisotropy of the Fermi sheet is increased. Finally, for our best fit Γ_3 FS ($t = 1$) the transition temperature of A_{1g} state ($T_c(A_{1g})$) is higher than that of E_{1g} state ($T_c(E_{1g})$), but the system is very close to the degeneracy point ($t \approx 0.85$) where $T_c(A_{1g}) = T_c(E_{1g})$. Thus application of a hydrodynamic pressure which decreases the crystal field t and restores "isotropy" may drive the system to a state with a single transition temperature $T_c = T_c(A_{1g}) = T_c(E_{1g})$, consistent with the Zhitomirskii and Luk'yanchuk scenario. [5] The role of the hexagonal crystal field is worth mentioning, since as we show in Fig. 3b the cylindrical crystal field lifts the spherical FS ($t = 0$) degeneracy of d-wave states and splits the transition temperatures corresponding to different irreducible representations. Therefore the situation of near degenerate states A_{1g} and E_{1g} is not realized when the pairing mainly takes place on the ellipsoidal Γ_2 FS. Analysis of the f-wave states shows that the E_{2u} irreducible representation, suggested to describe the superconducting state in Sauls' scenario, [1,18,34] is the one with the highest

transition temperature on Γ_3 FS but almost degenerate with A_{1u} representation (Fig. 2c). On the other hand, the transition temperature of A_{1u} state is significantly higher than that of E_{2u} on the Γ_2 sheet of FS (Fig. 3c).

III. GINZBURG-LANDAU COEFFICIENTS

Direct calculation of the GL coefficients incorporating aspects of the anisotropy of the FS is important for several reasons. The question of most current interest is the consistency of the Sauls E_{2u} scenario for the UPt_3 phase diagram. [1] This theory relies on the smallness of a particular term in the GL gradient free energy, which may be shown to destroy the isotropy of the tetracritical point in the 2D scenario. In the particular case of the E_{2u} representation, this term may be shown to vanish in cylindrical symmetry, and it is therefore hexagonal anisotropy alone which is responsible for the disagreement between the predictions of the E_{2u} scenario for the phase diagram and experiment. If the effect of the anisotropy could be shown to be quite small, i.e. the system were in this sense quite close to a cylindrically symmetric one, one would have considerably more confidence in the theory.

Before discussing this point in some detail, we remark however that other important physical information can be gleaned from a weak coupling calculation of the GL coefficients over the FS. Experimentally measurable quantities at the transition depend directly on combinations of the GL coefficients, e.g. for the specific heat jump, $\Delta C/C_N = \alpha^2/2\beta_1 T_c$. If sufficient independent measurements can be made to pin down the coefficients individually, and if the correct representation is known, comparison with weak-coupling calculations including the correct Fermi surface could in principle allow one to determine the size of strong-coupling corrections. This might in turn serve as a guide for theories of the UPt_3 normal state.

The form of the GL free energy density has been given in several places, e.g. Refs. 1,13. For the 2D representations in hexagonal symmetry it takes the form

$$f = \alpha|\bar{\eta}|^2 + \beta_1|\bar{\eta}|^4 + \beta_2|\bar{\eta}\bar{\eta}|^2 + \gamma_1|\bar{\eta}|^6 + \gamma_2|\bar{\eta}|^2|\bar{\eta}\bar{\eta}|^2 + \tag{20}$$

$$\sum_{i,j=x,y}\{\kappa_1 (\partial_i\eta_j)(\partial_i\eta_j)^* + \kappa_2 (\partial_i\eta_i)(\partial_j\eta_j)^* + \kappa_3 (\partial_i\eta_j)(\partial_j\eta_i)^* + \kappa_4 (\partial_z\eta_j)(\partial_z\eta_j)^*\}$$

with the order parameter given by the 2D vector

$$\bar{\eta} = (\eta_1, \eta_2) \tag{21}$$

that is for

$$\psi(\mathbf{k}) = \eta_1\phi_1(\mathbf{k}) + \eta_2\phi_2(\mathbf{k}) \tag{22}$$

in the case of even parity (Eq. (5)) and

$$d_\mu(\mathbf{k}) = \eta_1\varphi_1^\mu(\mathbf{k}) + \eta_2\varphi_2^\mu(\mathbf{k}) \tag{23}$$

for an odd parity (Eq. (6)), where $\phi_l(\mathbf{k})$ and $\varphi_l^\mu(\mathbf{k})$ are the polynomials listed in Tabs. I-III. In the spin-triplet states we have assumed that the $\mathbf{d}$ vector is real and oriented along the crystal direction $\hat{c}$ ($\hat{z}$-axis) by strong spin-orbit coupling in accordance with Sauls' scenario. [1] This conjecture leads to the identical forms of the GL functionals for both even and odd states. [34]

Expressions for the GL coefficients are straightforward to obtain through expansion of the Luttinger-Ward functional for the BCS superconductor in powers of the order parameter, and identification of the prefactors of the various invariants present in the phenomenological form in Eq. (18). One finds for the case of even parity

$$\alpha = N_0 \ln \frac{T}{T_c}$$

$$\beta_1 = 2\beta_2 = 2\beta_{BCS} \left\langle \phi_i^2 (\mathbf{k}) \phi_j^2 (\mathbf{k}) \right\rangle$$

$$\gamma_1 = \tfrac{2}{3}\gamma_2 = 2\gamma_{BCS} \left\langle \phi_i^2 (\mathbf{k}) \phi_j^4 (\mathbf{k}) \right\rangle$$

$$\kappa_1 = \kappa_{wc} \left\langle v_i^2 \phi_j^2 (\mathbf{k}) \right\rangle \tag{24}$$

$$\kappa_2 = \kappa_3 = \kappa_{wc} \left\langle v_i v_j \phi_i (\mathbf{k}) \phi_j (\mathbf{k}) \right\rangle$$

$$\kappa_4 = \kappa_{wc} \left\langle v_z^2 \phi_i^2 (\mathbf{k}) \right\rangle$$

$$\kappa_{123} = \kappa_{wc} \left\langle v_i^2 \phi_i^2 (\mathbf{k}) \right\rangle$$

where it is to be understood that $i \neq j$ $(i, j = x, y)$, $\kappa_{123} = \kappa_1 + \kappa_2 + \kappa_3$, and the constants are given by

$$\beta_{BCS} = \frac{7}{16}\zeta (3) \frac{N_0}{(\pi T_c)^2}$$

$$\gamma_{BCS} = -\frac{31}{128}\zeta (5) \frac{N_0}{(\pi T_c)^4} \tag{25}$$

$$\kappa_{wc} = \frac{7}{16}\zeta (3) \frac{N_0}{(\pi T_c)^2}$$

For odd parity these expression are analogous where we have to take into account that a product $\phi_i \phi_j$ is replaced by a scalar product $\bar{\varphi}_i \cdot \bar{\varphi}_j$.

Knowledge of the Fermi surface and of the basis functions for the various representations now allows one to evaluate, in principle, all coefficients of interest (Eq. (24)). There are several hidden problems in this analysis. The most serious has been alluded to above, namely our lack of knowledge of the relative pairing weight on each of the sheets of the

Fermi surface. As before, we approach this difficulty by assuming that pairing takes place either on the Γ_3 or the Γ_2 sheets of the Fermi surface, and discuss both cases separately. The second has to do with the choice of basis functions. We compare two different methods and calculate the coefficients for the expansion of the order parameter in the spherical harmonics and in the FS harmonics. Another complication arises from an infinite number of functions belonging to each irreducible representation in a crystal. Thus our choice of the $\phi_l(\mathbf{k})$ and $\bar{\varphi}_l(\mathbf{k})$ is perforce somewhat arbitrary. In this work we generally work with the lowest order polynomial functions for each representation. We can test to see whether the choice of higher order polynomials will greatly alter the size of the coefficients in Eq. (24) (it does not), but a more quantitative approach would allow the order parameter $\hat{\Delta}_k$ to adjust to the given angle-resolved density of states by taking a general linear combination of many such functions. This would have, for the FS harmonic representation particularly, the virtue of allowing for smoothing of singularities which inevitably result from the rapid changes of $\mathbf{v_k}$ over a complicated Fermi surface. Working with a single function $\phi_l(\mathbf{v_k})$ and $\varphi_l^{\mu}(\mathbf{v_k})$ is sufficient for our purposes, however, since the coefficients in Eq. (24) are always integrated over the full FS under consideration, and only the degree of hexagonal anisotropy should be important.

A special role in the topology of the $H-T$ phase diagram of the the 2D representations is played by the coefficient κ_2 (Eqs. (20), (24)) which mixes the gradients of the two components of the order parameter. The solution of the eigenvalue problem determining the critical field lines in the $H-T$ plane is analogous to a Schödinger equation for a charge moving in a magnetic field. The existence of a tetracritical point has been shown therefore to correspond to a level crossing, which cannot exist in the absence of a conserved quantum number. The κ_2 mixing terms correspond to a level repulsion (or hybridisation) term in this analogy, and thus prevent a crossing of the critical field lines for $\mathbf{H} \parallel \hat{\mathbf{c}}$.

By examining Table III, it is easy to see from Eq. (22) that the coefficient κ_2 in a cylindrically symmetric system, where $\mathbf{v} \parallel \mathbf{k}$, vanishes for E_{2u} symmetry whereas for the E_1 representations, $\kappa_2/\kappa_{wc}v_{F\perp}^2$ is of $\mathcal{O}(1)$. Similarly it is easy to check that $\kappa_1/\kappa_{wc}v_{F\perp}^2$ is of $\mathcal{O}(1)$

for both representations. Sauls' argument [1] is therefore that if hexagonal anisotropy effects are weak ($\kappa_2 \ll \kappa_1$), the critical fields may come so close as to mimic an apparent tetracritical point, even for $\mathbf{H} \parallel \hat{\mathbf{c}}$. To test this proposition, it is interesting to know not simply whether κ_2 is in fact much smaller than κ_1 when evaluated over the UPt_3 Fermi surface, but whether or not this result is "accidental" or due to the near cylindrical symmetry of the Fermi surface. Is the change in κ_2 due to hexagonal anisotropy in fact small? Sauls proposes that it is, and gives a perturbative analysis for a band structure of type given by Eq. (17), assuming a_3 small. In this case one finds $\kappa_2/\kappa_1 \simeq 0.1$. [36] It is however not clear that a perturbative analysis is applicable. Here we calculate κ_1, κ_2 numerically for the band given by Eq. (17), and display the results as a function of the anisotropy parameter a_3 in Fig. 4. In the calculation presented in Fig. 4a the order parameter was expressed in the spherical harmonics, whereas Fig. 4b shows the result for the FS harmonic representation of the gap function. The Γ_3 Fermi sheet is given by $a_3/(\varepsilon_F c^6) = 0.016$ (Table. IV) and the corresponding κ_1, κ_2 values are marked with a dotted line in Fig. 4. We read from Fig. 4a that $\kappa_2/\kappa_1 \simeq 0.46$ for the order parameter expressed by the spherical harmonics and from Fig. 4b that $\kappa_2/\kappa_1 \simeq 0.73$ for the FS harmonic expansion of the order parameter. Because of the cylindrical symmetry of Γ_2 FS, the κ_2 coefficient calculated over this FS sheet vanishes.

IV. CONCLUSIONS

We have tried to take crude features of the UPt_3 Fermi surface into account within a weak-coupling theory of unconventional superconductivity to see which order parameter symmetries are favored by Fermi surface structure alone. In the current philosophy, these are classified according to their angular momentum quantum numbers in the fictitious spherical system obtained when the ellipsoidal and hexagonal deformations of the "true" Fermi surface are "turned off". Within this scheme, we have examined states of p, and d, and f symmetry. Other important elements of the physics, such as the actual nature of the spin-orbit coupling and the range of the pairing, may also play major roles, but have been neglected here. The

lack of knowledge of a microscopic pairing mechanism–and consequent inability to specify the relative pairing weights on the various Fermi surface sheets–prevents us from drawing firm conclusions from an analysis of this type, but our results are suggestive.

It is worth observing that the few representations we have found to be stabilized by Fermi surface anisotropy are precisely those under active consideration as candidates for the UPt_3 order parameter: the two-dimensional representations E_{1g} and E_{2u} and the 1D representations A_{1u} and A_{1g}. Both of the 1D representations found are of interest in the accidentally degenerate representation scenario of Garg and co-workers, [3] which requires, however, mixing of nearly degenerate A-type and B-type representations. All of the latter are disfavored by the Fermi surface deformations we consider; our results do not therefore lend support to this model. The trivial representation A_{1g} corresponds to basis functions with the full symmetry of the Fermi surface, which typically are fully gapped. Such functions will be strongly supressed by local Coulomb interactions, which we do not consider here; they are by themselves ruled out by experiment. Exceptions occur if the system condenses in an A_{1g} state with nodes, or mixes with another representation supporting basis functions with nodes, as in the Zhitomirskii- Luk'yanchuk scenario. [5] The near degeneracy found in Figure 2b) for the A_{1g} and E_{1g} states for $t \simeq 0.85$, which is very close to the best fit to the Γ_3 Fermi surface sheet ($t = 1$), is some support for this picture.

We have attempted to account for our ignorance of the true distribution of the pair weights over the various Fermi surface sheets by examining models with pairing on the two sheets with highest density of states according to de Haas-van Alphen measurements, namely Γ_2 and Γ_3. As Γ_2 is nearly ellipsoidal but Γ_3 has strong hexagonal deformations, this choice has the additional virtue of crudely separating hexagonal and ellipsoidal variations. This may be of significance for current theories: for example, the hexagonal deformation appears to be important in stabilizing the E_{2u} representation. Confirmation of the E_{2u} model would therefore be indirect evidence for pairing primarily on the Γ_3 sheet. Such conclusions could be used as guides for microscopic pairing theories.

The scenario based on the E_{2u} representation due to Sauls [1] is based on the assumption that the level repulsion term in the Schrödinger-like equation for the critical field lines vanishes due to the proximity of the system to cylindrical symmetry. This term is proportional to the ratio of GL gradient coefficients $(\kappa_2/\kappa_1)^2$, [36] which vanishes in this limit for the E_{2u} state. We have calculated these coefficients over our model Fermi surfaces fit to LDA calculations and dHvA measurements, and find that this term is not small, but varies between .21 and .53, depending on our assumptions regarding the exact form of the basis functions. While the parametrization of the Fermi surface we have adopted is extremely simplistic, it has the virtue that one can discuss the proximity to cylindrical symmetry. What Figure 4 suggests is that the UPt_3 system may not really be regarded as close to cylindrically symmetric, and that therefore if calculations of the GL coefficients over the true Fermi surface produce a smaller value, [36] it should be regarded as coincidence. This undermines somewhat the attractiveness of the Sauls E_{2u} scenario, but of course does not constitute proof against it. One way in which this conclusion could be avoided is to have contributions to κ_2 which change sign on different Fermi surface sheets, leading to a smaller effective κ_2. This effect is indeed found in a calculation with the full UPt_3 LDA Fermi surface and a model with weight distributed equally over all sheets. [37]

ACKNOWLEDGMENTS

We are grateful to M. Norman and J. A. Sauls for many helpful discussions. One of us (G.H.) was partially supported by the Fulbright Foundation. Furthermore, M.S. would like to thank the Swiss Nationalfonds for support by a PROFIL fellowship.

REFERENCES

* new address: Yukawa Institute for Theoretical Physics, Kyoto University, Kyoto 606-01, Japan.

[1] J. A. Sauls, Adv. in Phys. **43**, 113 (1994).

[2] R. Joynt, V. P. Mineev, G. E. Volovik, and M. E. Zhitomirsky, Phys. Rev. **B42**, 2014 (1990).

[3] D. -C. Chen and A. Garg, Phys. Rev. Lett. **70**, 1689 (1993).

[4] K. Machida and M. Ozaki, Phys. Rev. Lett. **66**, 3293 (1991).

[5] M. E. Zhitomirskii and I. A. Luk'yanchuk, JETP Lett. **58**, 131 (1993).

[6] S. Adenwalla, S. W. Lin, Q. Z. Ran, Z. Zhao, J. B. Ketterson, J. A. Sauls, L. Taillefer, D. G. Hinks, M. Levy, and B. K. Sarma, Phys. Rev. Lett. **65**, 2298 (1990).

[7] K. Hasselbach, A. Lacerda, K. Behnia, L. Taillefer, J. Flouquet, and A. de Visser, J. Low Temp. Phys. **81**, 299 (1990).

[8] H. v. Löhneysen, T. Trappmann, and L. Taillefer, J. Magn. Magn. Mater. **108**, 49 (1992).

[9] M. Boukhny, G. L. Bullock, B. S. Shivaram, and D. G. Hinks, Phys. Rev. Lett. **73**, 1707 (1994).

[10] G. E. Volovik and L. P. Gorkov, Sov. Phys. JETP **61**, 843 (1985).

[11] E. Blount, Phys. Rev. **B32**, 2935 (1985).

[12] K. Ueda and T. M. Rice, Phys. Rev. **B31**, 7114 (1985).

[13] M. Sigrist and K. Ueda, Rev. Mod. Phys. **63**, 239 (1991).

[14] L. Taillefer, R. Newbury, G. G. Lonzarich, Z. Fisk, and J. L. Smith, J. Magn. Magn. Mater. **63&64**, 372 (1987).

[15] T. Oguchi, A. J. Freeman, and G. W. Crabtree, J. Magn. Magn. Mater. **63&64**, 645 (1987).

[16] M. R. Norman, R. C. Albers, A. M. Boring, and N. E. Christensen, Solid State Commun. **68**, 245 (1988).

[17] R. Joynt, Sup. Sci. Tech. **1**, 210 (1988).

[18] D. Hess, T. Tokoyasu and J. A. Sauls, J. Phys. Condens. Matter **1**, 8135 (1989).

[19] S. M. Hayden, L. Taillefer, C. Vettier, and J. Flouquet, Phys. Rev. **B46**, 8675 (1992).

[20] K. Machida, Prog. Theor. Phys. Suppl. **108**, 229 (1992).

[21] K. A. Park and R. Joynt, Phys. Rev. **B53**, 12346 (1996).

[22] D. S. Jin, A. Husmann, T. F. Rosenbaum, T. E. Steyer and K. T. Faber, Phys. Rev. Lett. **78**, 1775 (1997).

[23] J. A. Sauls, Phys. Rev. **B53**, 8543 (1996).

[24] B. Lussier, L. Taillefer, W. J. L. Buyers, T. E. Mason and T. Petersen Phys. Rev. **B54**, R6873 (1996); see also E. D. Isaacs, P. Zschack, C. L. Broholm, C. Burns, G. Aeppli, A. P. Ramirez, T. T. M. Palstra, R. W. Erwin, N. Stücheli, and E. Bucher, Phys. Rev. Lett. **75**, 1178 (1995).

[25] H. Tou, Y. Kitaoka, K. Asayama, N. Kimura, Y. Onuki, E. Yamamoto and K. Maezawa, Phys. Rev. Lett. **77**, 1374 (1996).

[26] K. Machida and T. Ohmi, J. Phys. Soc. Japan Lett. **65**, 3456 (1996); T. Ohmi and K. Machida, J. Phys. Soc. Japan **65**, 4018 (1996).

[27] C.H. Choi and J.A. Sauls, Phys. Rev. Lett. **66**, 484 (1991); Phys. Rev. **B48** 13684 (1993).

[28] L. Taillefer and G. G. Lonzarich, Phys. Rev. Lett. **60**, 1570 (1988).

[29] R. A. Fisher, S. Kim, B. F. Woodfield, N. E. Philips, L. Taillefer, K. Hasselbach, J. Flouquet, A. L. Giorgi, and J. L. Smith, Phys. Rev. Lett. **62**, 1411 (1989).

[30] J. W. Serene and D. Rainer, Phys. Rep. **101**, 221 (1983).

[31] P. B. Allen, Phys. Rev. **B13**, 1416 (1976).

[32] W. H. Butler and P. B. Allen, in *Superconductivity in d- and f- band metals*, New York: Plenum Press, 1977.

[33] M. R. Norman and P. J. Hirschfeld, Phys. Rev. **B53**, 5706 (1996).

[34] T. A. Tokuyasu, D. W. Hess, and J. A. Sauls, Phys. Rev. **B41**, 8891 (1990).

[35] R. C. Albers, A. M. Boring, and N. E. Christensen, Phys. Rev. **B33**, 8116 (1986).

[36] V. Vinokur, J. A. Sauls, and M. R. Norman, private communication; Bull. Am. Phys. Soc. 39, 592 (1994).

[37] M. R. Norman and J. A. Sauls, private communication.

TABLES

TABLE I. Basis functions for the gap function: p-wave

l	*Irreducible representation* Γ	$\bar{\varphi}_l(\mathbf{k})$	*degenerate with*
1	A_{1u}	$\hat{\mathbf{z}}k_z$	
2	A_{1u}	$\hat{\mathbf{x}}k_x + \hat{\mathbf{y}}k_y$	$E_{1u}(\mathbf{d} \parallel \hat{z})$
3	A_{2u}	$\hat{\mathbf{x}}k_y - \hat{\mathbf{y}}k_x$	$E_{1u}(\mathbf{d} \parallel \hat{z})$
4	E_{1u}	$\hat{\mathbf{z}}k_x$	
5		$\hat{\mathbf{z}}k_y$	
6	E_{1u}	$\hat{\mathbf{x}}k_z$	$A_{1u}(\mathbf{d} \parallel \hat{z})$
7		$\hat{\mathbf{y}}k_z$	
8	E_{2u}	$\hat{\mathbf{x}}k_x - \hat{\mathbf{y}}k_y$	$E_{1u}(\mathbf{d} \parallel \hat{z})$
9		$\hat{\mathbf{x}}k_y + \hat{\mathbf{y}}k_x$	

TABLE II. Basis functions for the gap function: d-wave

l	*Irreducible representation* Γ	$\phi_l(\mathbf{k})$
1	A_{1g}	$2k_z^2 - k_x^2 - k_y^2$
2	E_{1g}	$k_x k_z$
3		$k_y k_z$
4	E_{2g}	$k_x^2 - k_y^2$
5		$2k_x k_y$

TABLE III. Basis functions for the gap function: f-wave

l	*Irreducible representation* Γ	$\bar{\varphi}_l(\mathbf{k})$	*degenerate with*
10	A_{1u}	$\hat{\mathbf{z}}k_z(2k_z^2-3k_x^2-3k_y^2)$	
11	A_{1u}	$(\hat{\mathbf{x}}k_x+\hat{\mathbf{y}}k_y)(4k_z^2-k_x^2-k_y^2)$	$E_{1u}(\mathbf{d}\parallel\hat{z})$
12	A_{2u}	$(\hat{\mathbf{x}}k_y-\hat{\mathbf{y}}k_x)(4k_z^2-k_x^2-k_y^2)$	$E_{1u}(\mathbf{d}\parallel\hat{z})$
13	B_{1u}	$\hat{\mathbf{z}}(k_x^3-3k_y^2k_x)$	
14	B_{1u}	$\hat{\mathbf{x}}k_z(k_x^2-k_y^2)+2\hat{\mathbf{y}}k_xk_yk_z$	$E_{2u}(\mathbf{d}\parallel\hat{z})$
15	B_{2u}	$\hat{\mathbf{z}}(k_y^3-3k_x^2k_y)$	
16	B_{2u}	$\hat{\mathbf{y}}k_z(k_x^2-k_y^2)+2\hat{\mathbf{x}}k_xk_yk_z$	$E_{2u}(\mathbf{d}\parallel\hat{z})$
17	E_{1u}	$\hat{\mathbf{z}}k_x(4k_z^2-k_x^2-k_y^2)$	
18		$\hat{\mathbf{z}}k_y(4k_z^2-k_x^2-k_y^2)$	
19	E_{1u}	$\hat{\mathbf{x}}k_z(2k_z^2-3k_x^2-3k_y^2)$	$A_{1u}(\mathbf{d}\parallel\hat{z})$
20		$\hat{\mathbf{y}}k_z(2k_z^2-3k_x^2-3k_y^2)$	
21	E_{1u}	$\hat{\mathbf{x}}k_z(k_x^2-k_y^2)-2\hat{\mathbf{y}}k_xk_yk_z$	$E_{2u}(\mathbf{d}\parallel\hat{z})$
22		$\hat{\mathbf{y}}k_z(k_x^2-k_y^2)-2\hat{\mathbf{x}}k_xk_yk_z$	
23	E_{2u}	$\hat{\mathbf{z}}k_z(k_x^2-k_y^2)$	
24		$2\hat{\mathbf{z}}k_xk_yk_z$	
25	E_{2u}	$(\hat{\mathbf{x}}k_x-\hat{\mathbf{y}}k_y)(4k_z^2-k_x^2-k_y^2)$	$E_{1u}(\mathbf{d}\parallel\hat{z})$
26		$(\hat{\mathbf{x}}k_y+\hat{\mathbf{y}}k_x)(4k_z^2-k_x^2-k_y^2)$	
27	E_{2u}	$\hat{\mathbf{x}}(k_x^3-3k_y^2k_x)$	$B_{1u}(\mathbf{d}\parallel\hat{z})$
28		$\hat{\mathbf{y}}(k_x^3-3k_y^2k_x)$	
29	E_{2u}	$\hat{\mathbf{x}}(k_y^3-3k_x^2k_y)$	$B_{2u}(\mathbf{d}\parallel\hat{z})$
30		$\hat{\mathbf{y}}(k_y^3-3k_x^2k_y)$	

TABLE IV. The functions and the coefficients used in fitting Γ_2 and Γ_3 energy bands, $c = 4.9027\mathring{A}$ is the z-axis lattice constant (Ref. 35).

i	a_i	Γ_2	Γ_3	$f_i(\mathbf{k})$
1	$a_1/(\varepsilon_F c^2)$	0.466	0.157	k_z^2
2	$a_2/(\varepsilon_F c^2)$	0.951	0.241	$k_x^2 + k_y^2$
3	$a_3/(\varepsilon_F c^6)$	0	0.016	$\left(k_y^3 - 3k_x^2 k_y\right)^2$

FIGURE CAPTIONS

Fig. 1. Γ_3 (solid line) and Γ_2 (dashed line) Fermi sheet plot in the symmetry plane: a) $K\Gamma M$, b) $L\Gamma M$, c) $H\Gamma K$.

Fig. 2. The hexagonal crystal field t effect on the critical temperature of the a) p-wave states, b) d-wave states, c) f-wave states. $t = 0$ corresponds to isotropic, $t = 1$ to best fit dHvA-LDA Γ_3 Fermi surface.

Fig. 3. The cylindrical crystal field t effect on the critical temperature of the a) p-wave states, b) d-wave states, c) f-wave states. $t = 0$ corresponds to isotropic, $t = 1$ to best fit dHvA-LDA Γ_2 Fermi surface.

Fig. 4. Normalized κ_1 (solid line) and κ_2 (dashed line) stiffness coefficients as the functions of the normalized FS hexagonal anisotropy parameter a_3: a) spherical harmonics representation, b) FS harmonics representation. The dotted line corresponds to the value $a_3/\epsilon_F c^6 = 0.016$ obtained by a fit to the Γ_3 Fermi surface sheet.

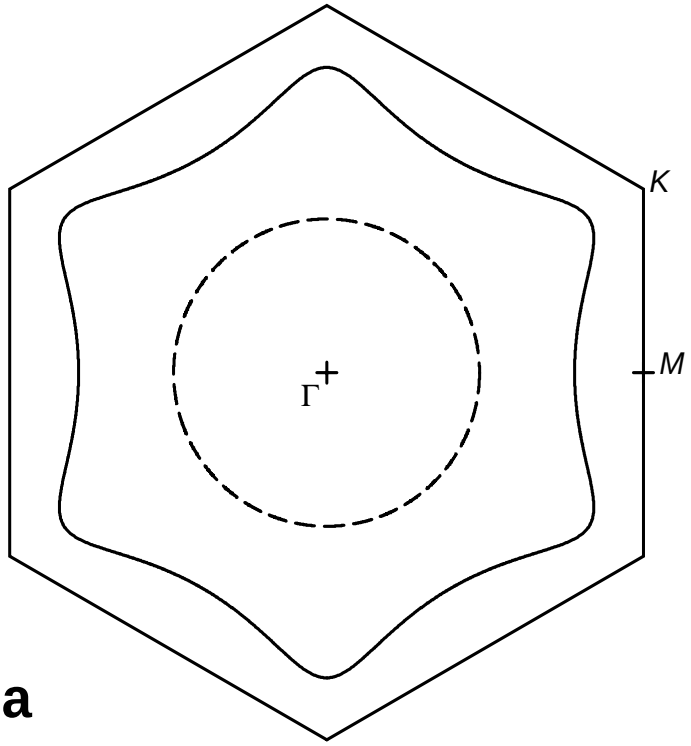
K
M
Γ+
a

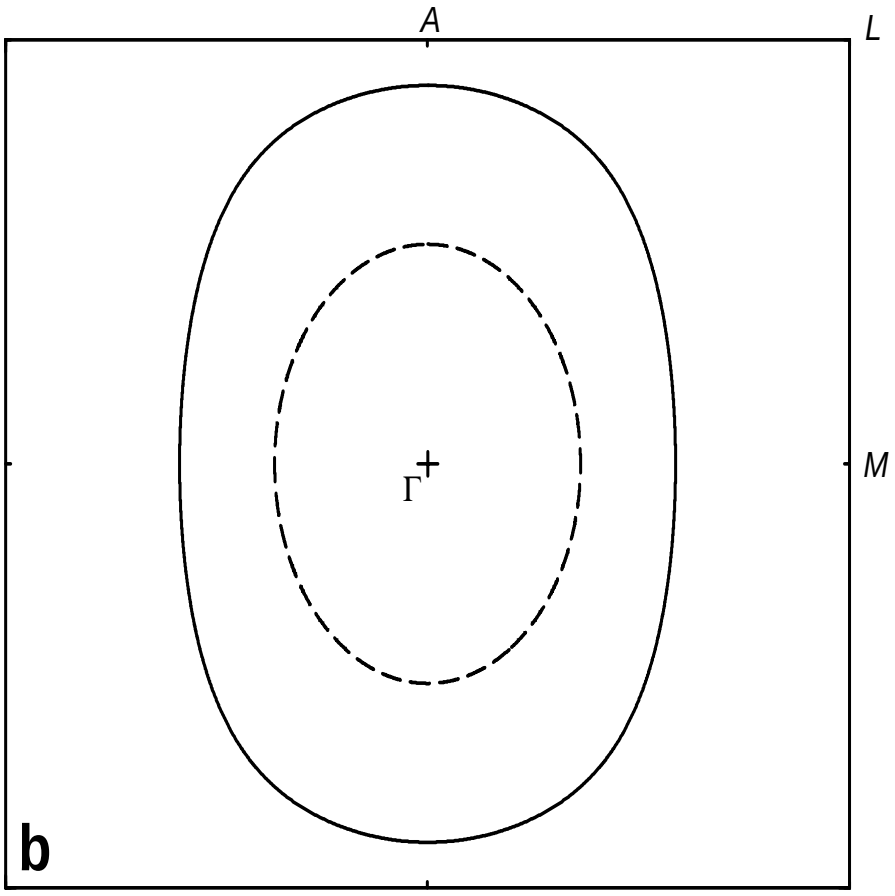
A
L
M
Γ+
b

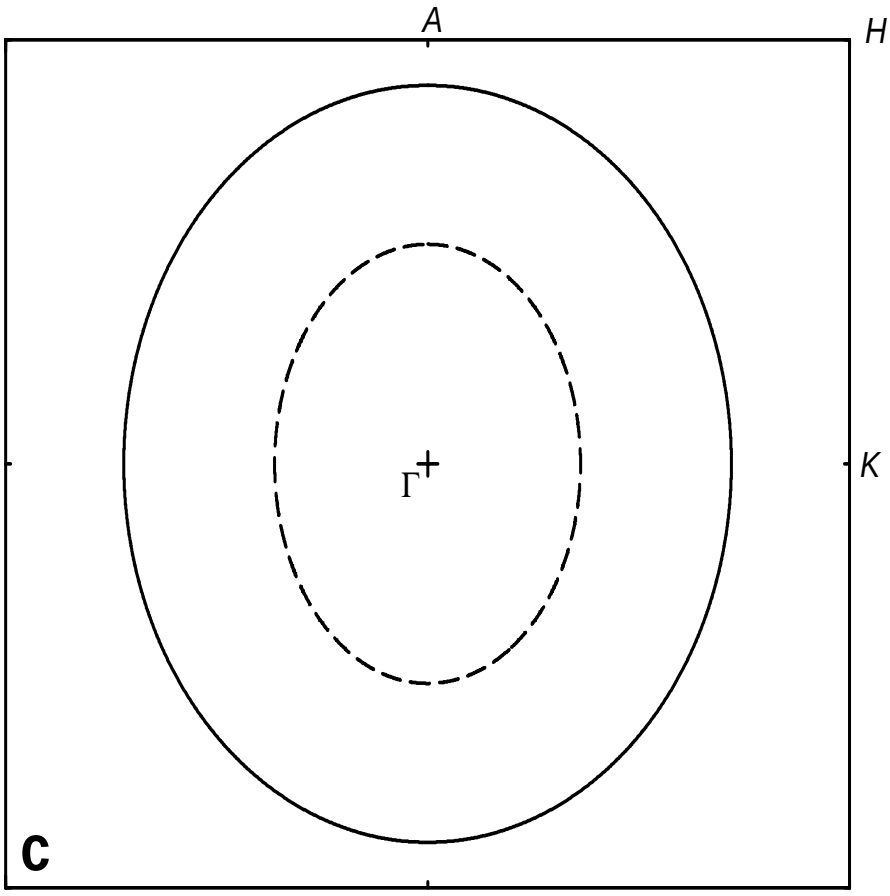
A
H
K
Γ+
c

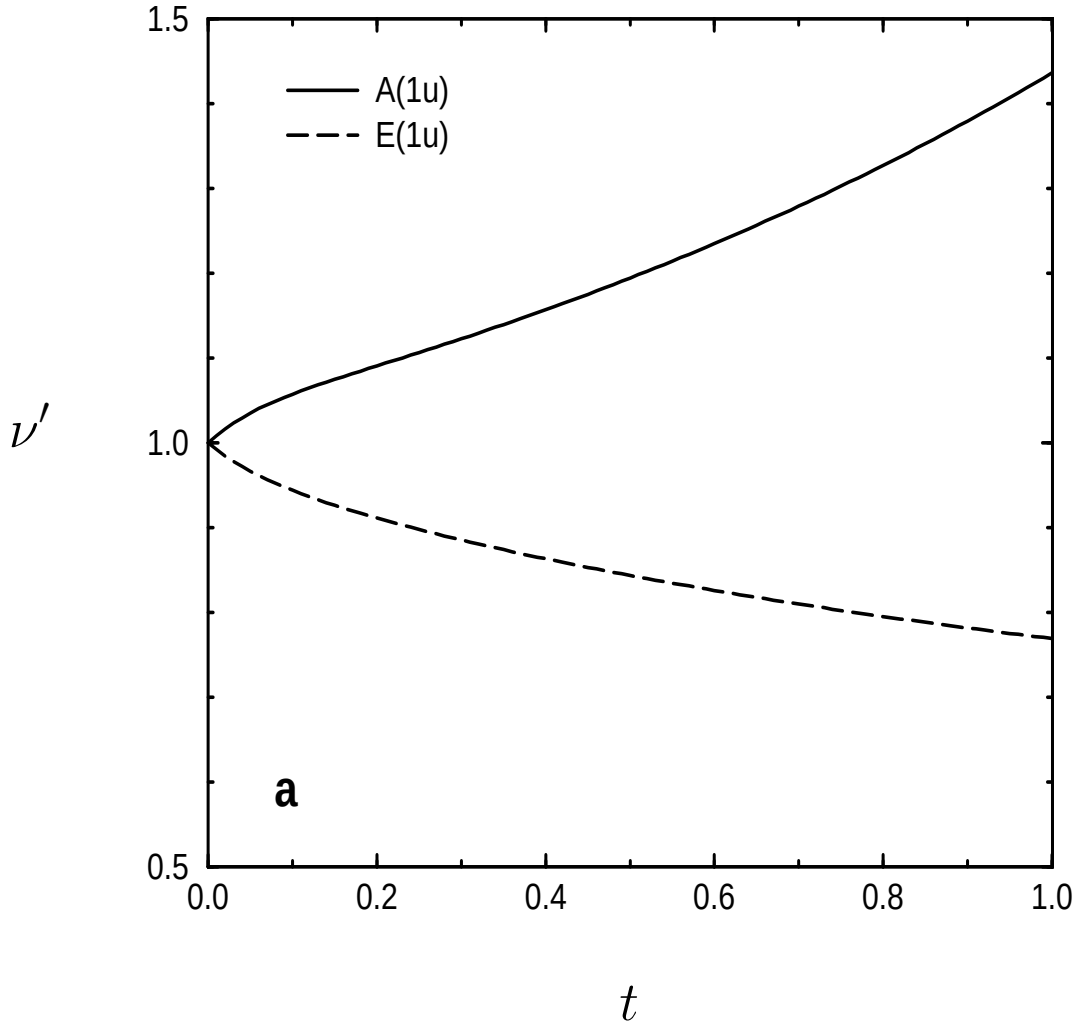
1.5
1.0
0.5
A(1u)
E(1u)
a
0.0
0.2
0.4
0.6
0.8
1.0
ν'
t

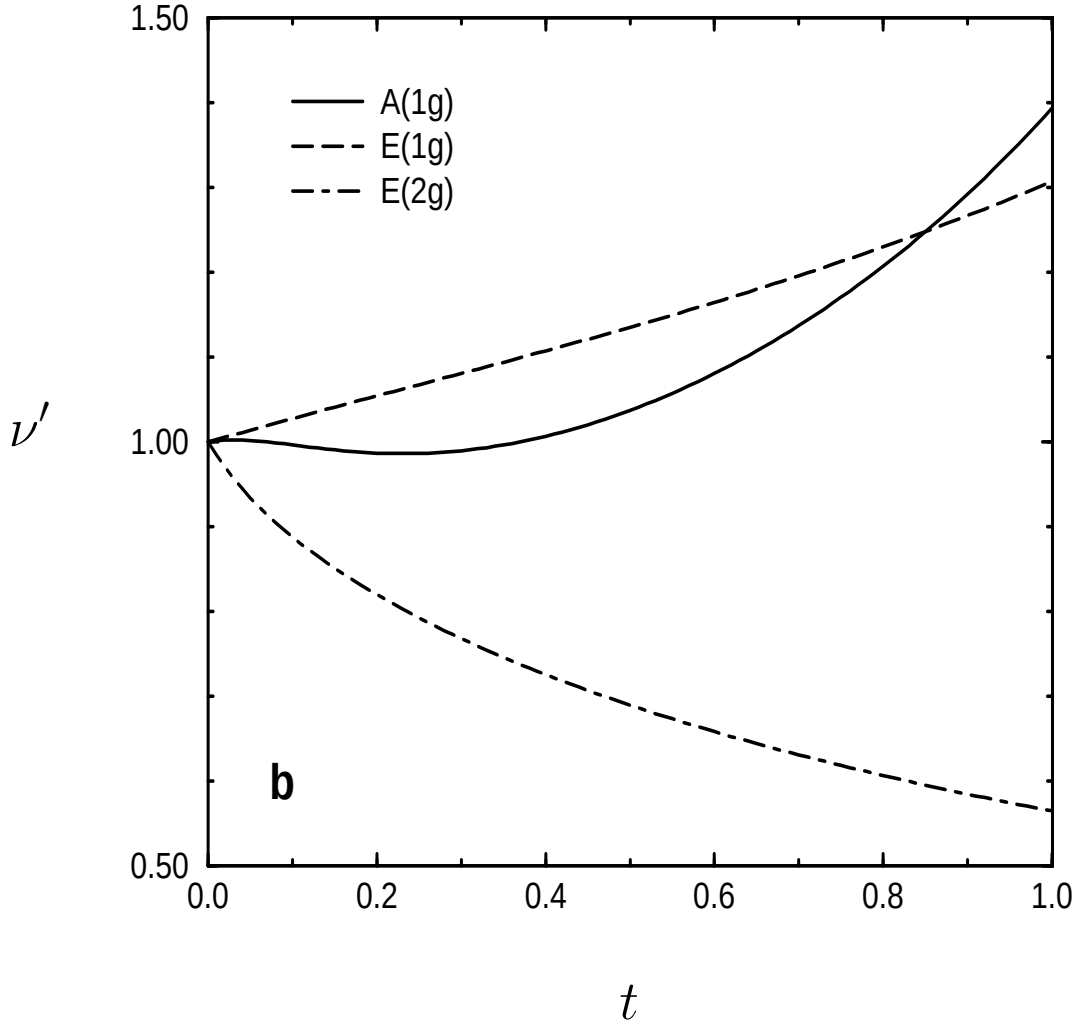
1.50
1.00
0.50
0.0
0.2
0.4
0.6
0.8
1.0
A(1g)
E(1g)
E(2g)
b
ν'
t

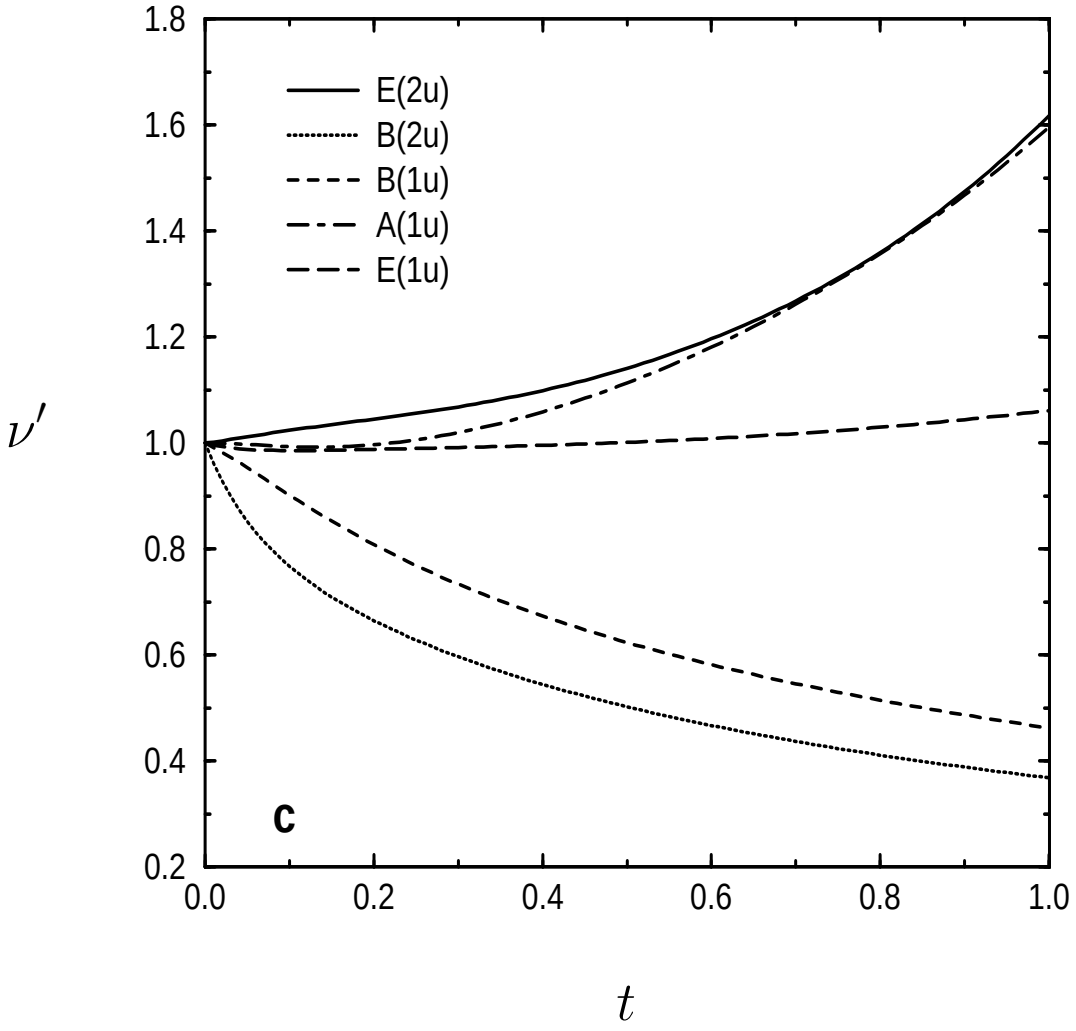
E(2u)
B(2u)
B(1u)
A(1u)
E(1u)
c
1.8
1.6
1.4
1.2
1.0
0.8
0.6
0.4
0.2
0.0
0.2
0.4
0.6
0.8
1.0
ν'
t

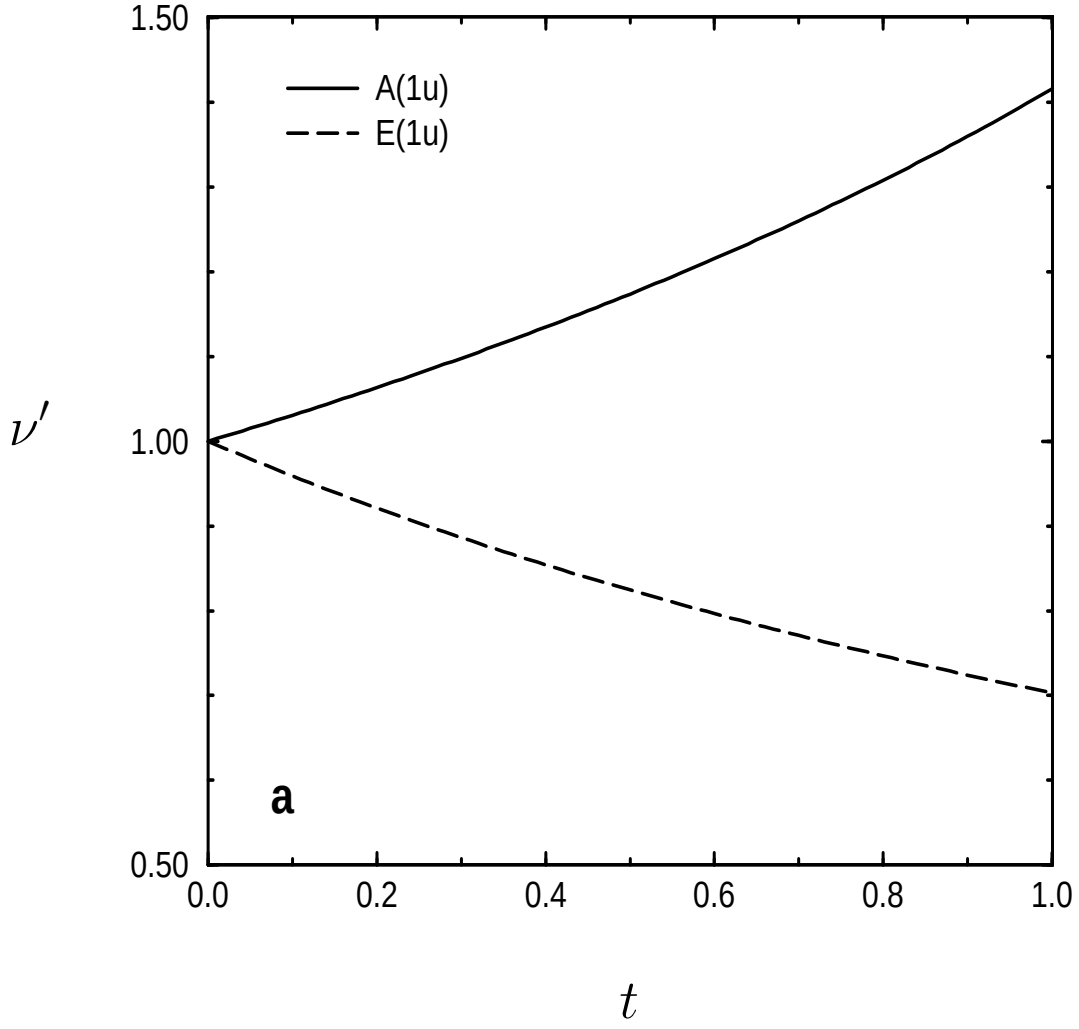
1.50
1.00
0.50
0.0
0.2
0.4
0.6
0.8
1.0
A(1u)
E(1u)
a
ν'
t

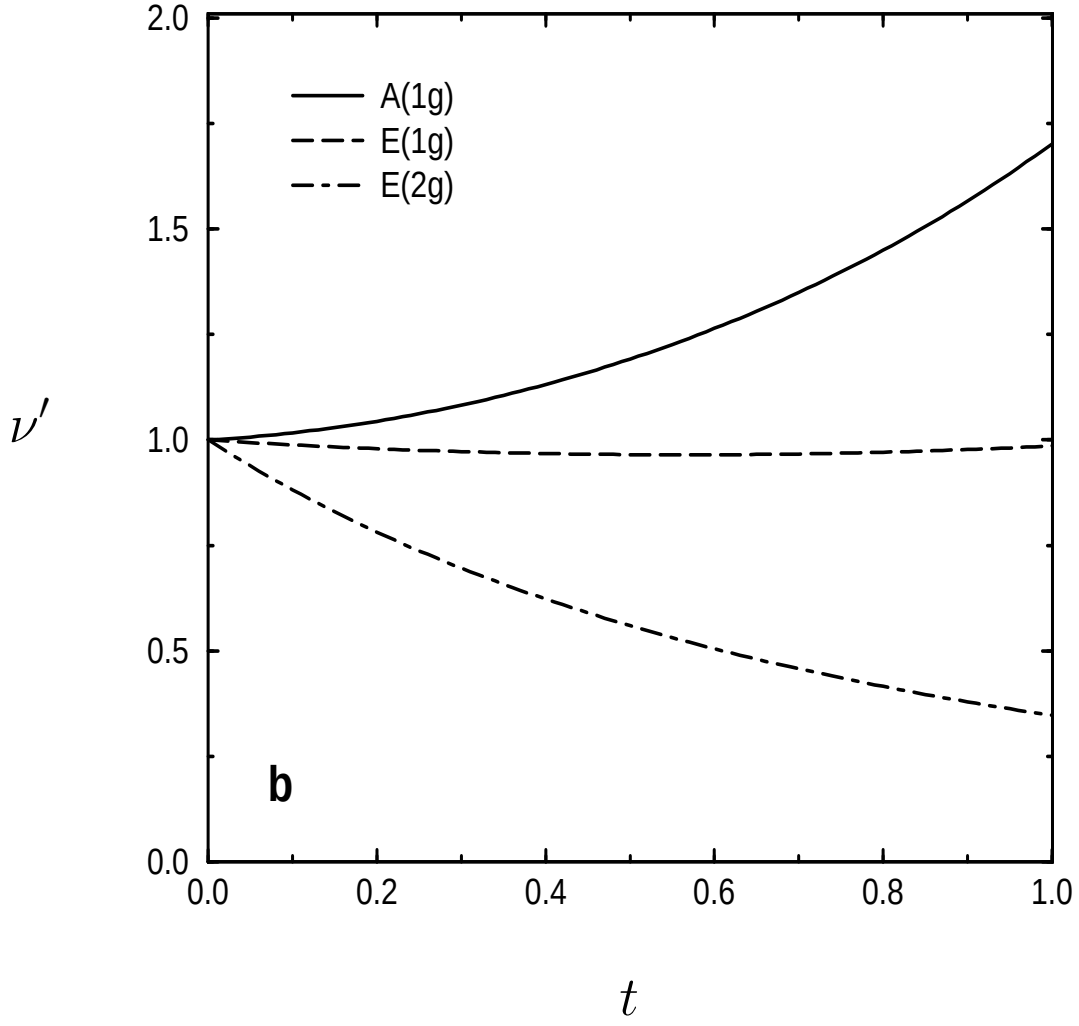
2.0
1.5
1.0
0.5
0.0
0.0
0.2
0.4
0.6
0.8
1.0
A(1g)
E(1g)
E(2g)
b
ν'
t

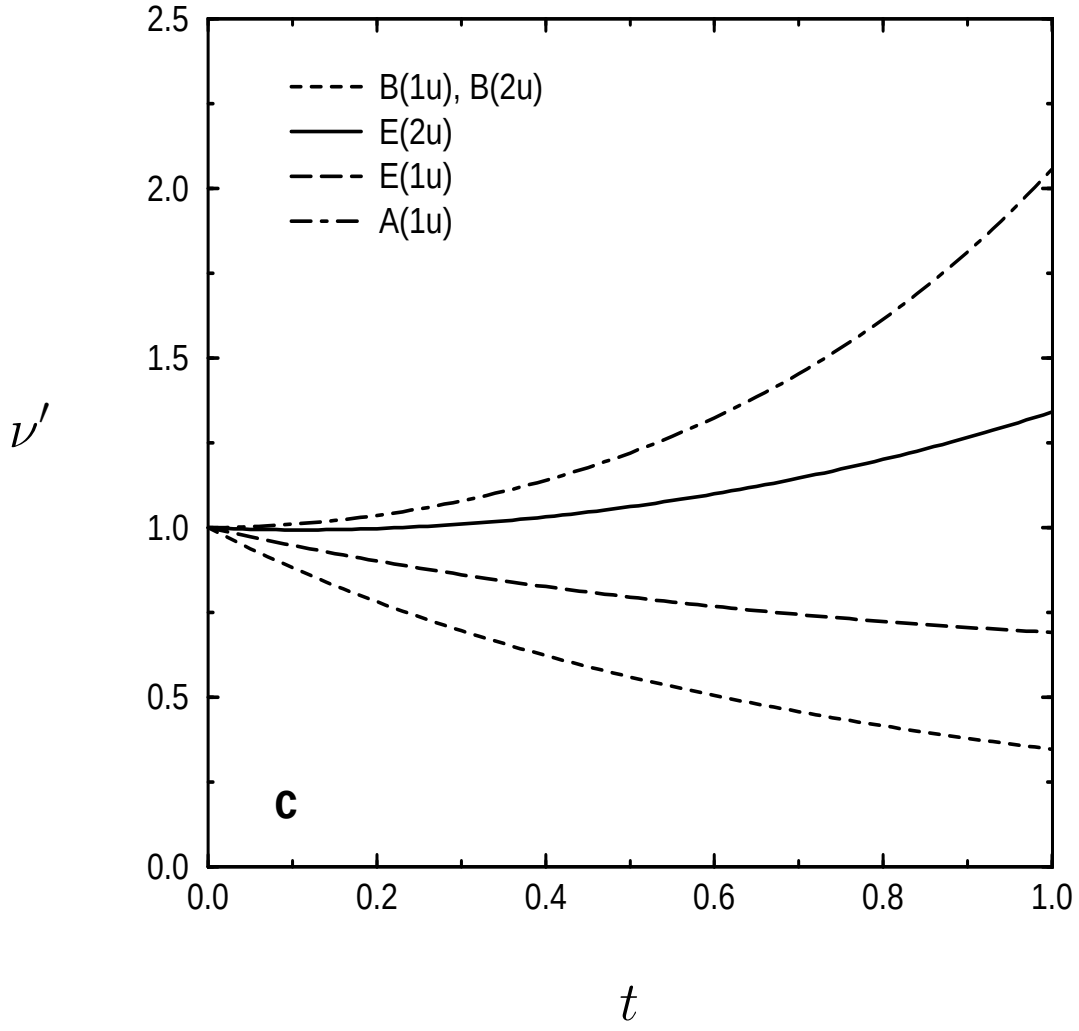
B(1u), B(2u)
E(2u)
E(1u)
A(1u)
c
2.5
2.0
1.5
1.0
0.5
0.0
0.0
0.2
0.4
0.6
0.8
1.0
ν'
t

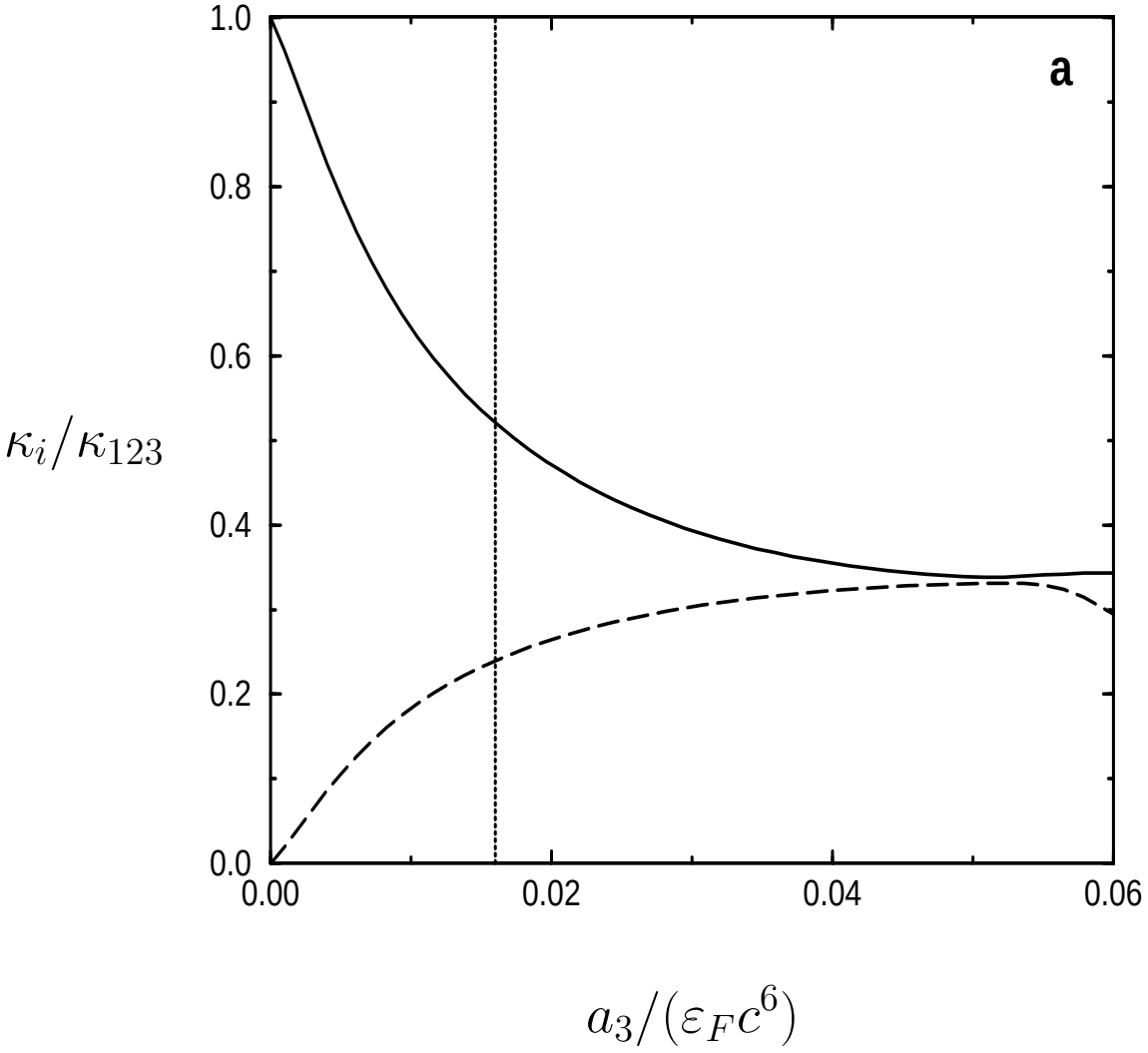
a
1.0
0.8
0.6
0.4
0.2
0.0
0.00
0.02
0.04
0.06
κ_i/κ_{123}
$a_3/(\varepsilon_F c^6)$

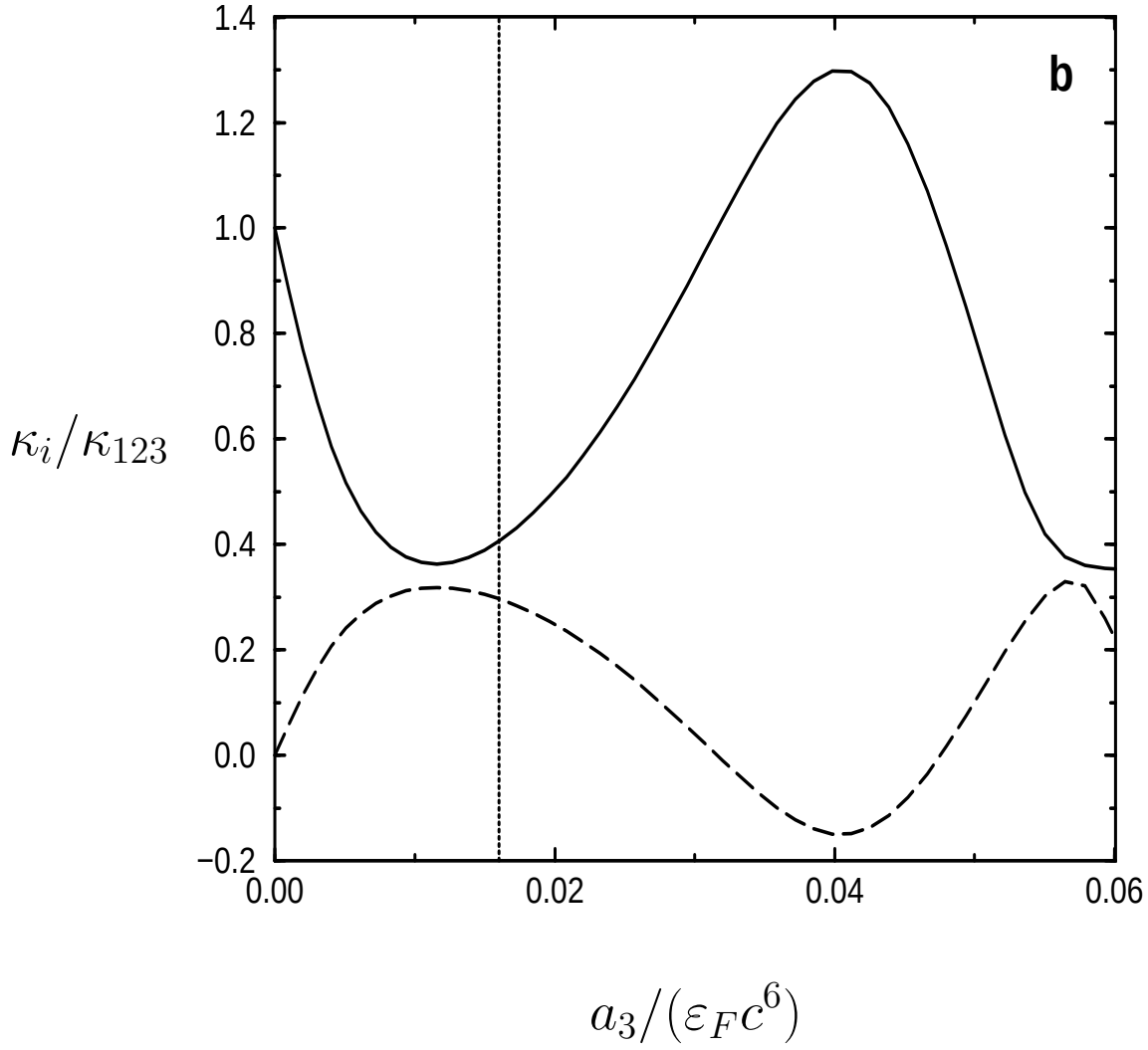
b
1.4
1.2
1.0
0.8
0.6
0.4
0.2
0.0
−0.2
0.00
0.02
0.04
0.06
κ_i/κ_{123}
$a_3/(\varepsilon_F c^6)$